INL/CON-08-15014
PREPRINT

The Discrete Equation Method (DEM) for Fully Compressible Two-Phase Flows in Ducts of Spatially Varying Cross-Section

ICONE 17

Ray A. Berry
Richard Saurel
Tamara Grimmett

July 2009

The INL is a
U.S. Department of Energy
National Laboratory
operated by
Battelle Energy Alliance

Proceedings of the 17th International Conference on Nuclear Engineering
ICONE17
July 12-16, 2009, Brussels, Belgium

ICONE17-75544

THE DISCRETE EQUATION METHOD (DEM) FOR FULLY COMPRESSIBLE TWO-PHASE FLOWS IN DUCTS OF SPATIALLY VARYING CROSS-SECTION

Ray A. Berry
Idaho National Laboratory
Idaho Falls, Idaho, 83415-3840 USA

Richard Saurel
Ecole Polytechnique Univeristaire de Marseille
Marseille, France

Tamara Grimmett
Idaho National Laboratory
Idaho Falls, Idaho, USA

ABSTRACT

Typically, multiphase modeling begins with an averaged system of (ill-posed) partial differential equations then discretizes this system to form a numerical scheme. Assuming that the ill-posedness problem is avoided by using a well-posed formulation such as the seven-equation model, this presents problems for the numerical approximation of non-conservative terms at discontinuities (interfaces, shocks) as well as unwieldy treatment of fluxes with seven waves. To solve interface problems without conservation errors and to avoid this questionable determination of average variables and the numerical approximation of the non-conservative terms associated with 2-velocity mixture flows a new homogenization method known as the Discrete Equations Method (DEM) [1] is employed. Contrary to conventional methods, the averaged equations for the mixture are not used, and this method directly obtains a well-posed discrete equation system from the single-phase system to produce a numerical scheme which accurately computes fluxes for arbitrary numbers of phases and solves non-conservative products. The method effectively uses a sequence of single phase Riemann equation solves. Phase interactions are accounted for by Riemann solvers at each interface. Flow topology can change with changing expressions for the fluxes. Non-conservative terms are correctly approximated. Some of the closure relations missing from the traditional approach are automatically obtained. Lastly, we identify the continuous equation system resulting from discrete equations by taking the continuous limit with weak wave assumptions. As a first step toward implict integration of the DEM method in multidimensions, in this paper we construct a DEM model for the flow of two compressible phases in 1-D ducts of spatially varying cross-section to test this approach. To relieve time step size restrictions due to stiffness and to achieve tighter coupling of equations, a fully implicit time integration method will eventually replace this explicit integration. For the first time, we demonstrate on a converging-diverging two-phase nozzle that this well-posed, 2 pressure, 2 velocity DEM model can be integrated to a meaningful steady-state with both phases treated as compressible.

INTRODUCTION

Typically, multiphase modeling begins with an averaged or homogenized system of partial differential equations (which are traditionally ill-posed) then discretizes this system to form a numerical scheme. This presents problems for the numerical approximation of non-conservative terms at discontinuities (such as interfaces and shocks) as well as the unwieldy treatment of fluxes with seven waves. To solve interface problems without conservation errors and to avoid this questionable determination of average variables and the numerical approximation of the non-conservative terms in

conjunction with 2-velocity mixture flows we employ a new homogenization method known as the Discrete Equations Method (DEM) [1]. Contrary to conventional methods, the averaged equations for the mixture are not used, and this method directly obtains a (well-posed) discrete equation system from the single-phase system to produce a numerical scheme which accurately computes fluxes for arbitrary numbers of phases and solves non-conservative products. The method effectively uses a sequence of single phase Riemann equation solves. Phase interactions are accounted for by Riemann solvers at each interface. Flow topology can change with changing expressions for the fluxes. Non-conservative terms are correctly approximated. Some of the closure relations missing from the traditional approach are automatically obtained. Lastly, we can sometimes identify the continuous system induced by the discrete equation. This can be very useful from a theoretical standpoint. In this paper we outline the construction of a DEM model for 1-D flow of two compressible phases in ducts of spatially varying cross-section to test this approach. For the first time, we demonstrate on a converging-diverging two-phase nozzle that this well-posed 2-pressure, 2-velocity model can be integrated to a meaningful steady-state with both phases treated as compressible. In this first attempt, we include a simple mass transfer model and postpone investigation of general mass transfer between multiple compressible phases through development of a Reactive Riemann solver (RDEM) [2,3] to a later date.

Simple, efficient and robust algorithms are needed to solve the well-posed models. The various ingredients employed in the methods to be developed should be general enough to consider future extensions to problems involving complex multiphysics. Using the fractional step methods typically applied (and often miss-applied) to calculate these types of initial value problems, consisting of different types of physics with multiple time-scales, some of which should be treated implicitly, requires some precautionary measures to avoid splitting and condi-tioning errors. For this initial test reported here we utilized explicit time integration. In the future, to relieve time step restrictions due to stiffness and to achieve tighter coupling of the equations, we believe that a fully implicit treatment may not only be advantageous, but necessary. An appropriate fully implicit approach will allow integration over the fast time scales for slow-transient flows. [We anticipate that using a Jacobian-Free Newton-Krylov method with physics-based preconditioning will allow tightly coupled solutions of the multiphysics phenomena inherent in nuclear reactor core applications.] Toward that objective, a significant effort has been expended toward development of a method of lines (MOL) or semidiscrete method [4] approach to the integration of the equation system. With the MOL we discretize separately the space and time domains, effectively converting to a large system of ordinary differential equations (ODE) that can be integrated with previously developed, highly refined special purpose software. [Though not documented in this paper, we are currently incorporating the 1-D variable area, two-phase DEM algorithm to be described below into this framework.] Thus this explicit model described below serves as a necessary beginning for the subsequent implicit methods development. We will test and report on the fully implicit integration of this system at a later date.

NOMENCLATURE

ρ density,

$\vec{u}$ velocity vector,

$\vec{u}_I$ local interfacial velocity,

P pressure,

E total energy: $E = e + \dfrac{\vec{u}\cdot\vec{u}}{2}$,

e internal energy.

THE DEM METHOD

We will assume here that each phase obeys the single phase Euler equations

$$\begin{aligned} &\frac{\partial \rho}{\partial t} + div(\rho\vec{u}) = 0 \\ &\frac{\partial \rho\vec{u}}{\partial t} + div(\rho\vec{u}\otimes\vec{u}) + grad(P) = 0 \\ &\frac{\partial \rho E}{\partial t} + div((\rho E + P)\vec{u}) = 0\,. \end{aligned} \tag{1}$$

Each phase is characterized by its phase function X_k [3] that obeys the evolution equation

$$\frac{\partial X_k}{\partial t} + \vec{u}_I\ grad(X_k) = 0 \tag{2}$$

where $\vec{u}_I$ represents the local interfacial velocity.

The DEM proceeds in a sequence of steps:

- fluid selection,
- integration over a control volume,
- determination of the phase contacts at cell boundaries,
- determine cell face fluxes and time integrate equations.

The **first step** consists in the fluid selection. We multiply the Euler equations, corresponding to a system of conservation laws by the characteristic (or phase) function

$$X_k\left(\frac{\partial U}{\partial t}+div(F)\right)=0$$

where the extended system of conservative variables (we have also included Eqn. (2)) is

$$U=\left(1,\rho,\rho\vec{u},\rho E\right)^T$$

and corresponding fluxes are

$$F\left(U\right)=\left(0,\rho\vec{u},\rho\vec{u}\otimes\vec{u}+P\overline{I},(\rho E+P)\vec{u}\right)^T .$$

After some manipulations we obtain

$$\frac{\partial X_k U}{\partial t}+div(X_k F)=(F-\vec{u}_I U)grad(X_k) . \quad (3)$$

The **second step** consists in the space integration of this equation, or

$$\int_V\left(\frac{\partial X_k U}{\partial t}+div(X_k F)\right)dV=\int_V(F-\vec{u}_I U)grad(X_k)dV . \quad (4)$$

The control volume being time invariant, the first term becomes

$$\int_V\frac{\partial X_k U}{\partial t}dV=\frac{\partial}{\partial t}\int_V X_k U dV=\frac{\partial V\left\langle X_k U\right\rangle}{\partial t} \quad (5)$$

with the following definition of cell averages

$$\left\langle X_k U\right\rangle=\frac{1}{V}\int_V X_k U dV .$$

The second term can be transformed using the Gauss theorem

$$\int_V div(X_k F)dV=\int_S X_k F\cdot\vec{n}dS .$$

This surface integral transforms to a sum of fluid surface integrals and solid surface integrals

$$\int_S X_k F\cdot\vec{n}dS=\int_{S_f} X_k F\cdot\vec{n}dS+\int_{S_s} X_k F\cdot\vec{n}dS .$$

The integral over fluid surfaces needs particular attention and will be achieved with the DEM. The solid surface integral can be simplified by noting that the flux expresses

$$\int_{S_s} X_k F\cdot\vec{n}dS=\int_{S_s} X_k\begin{pmatrix}0\\ \rho\vec{u}\\ \rho\vec{u}\otimes\vec{u}+P\overline{I}\\ (\rho E+P)\vec{u}\end{pmatrix}\cdot\vec{n}dS .$$

By using boundary conditions on solid surfaces we get

$$\int_{S_s} X_k\begin{pmatrix}0\\ \rho\vec{u}\\ \rho\vec{u}\otimes\vec{u}+P\overline{I}\\ (\rho E+P)\vec{u}\end{pmatrix}\cdot\vec{n}dS=\begin{pmatrix}0\\ 0\\ \int_{S_s} X_k P\vec{n}dS\\ 0\end{pmatrix}.$$

Consider the following varying cross-section as shown in Fig. 1.

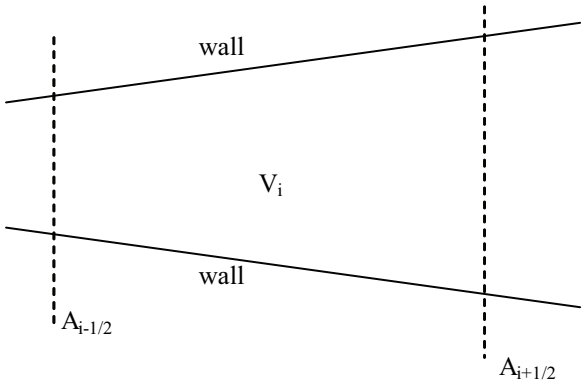

Figure 1. Cell volume, flow areas, and walls

Part of the wall is occupied by phase 1, the rest being occupied by phase 2. We assume that phase 1 is occupying the upper wall with the same concentration as with the lower wall. The pressure of phase 1 acts only on a part of the wall. Thus we have to compute

$$\int_{S_s} X_k P\vec{n}dS=\int_{S_{sk}} P_k\vec{n}dS ,$$

where s_{sk} represents the wall surface occupied by phase k.

Assuming the pressure is uniform in the given phase

$$\int_{S_{sk}} P_k\vec{n}dS=-\int_{Complement\ of\ S_{sk}} P_k\vec{n}dS .$$

Thus,

$$\int_{S_{sk}} P_k\vec{n}dS=-P_k(A_{k,out}-A_{k,in})\vec{i} .$$

The two surfaces $A_{k_{out}}$ and $A_{k_{in}}$ are included in the two phase control volume as shown in Fig. 2.

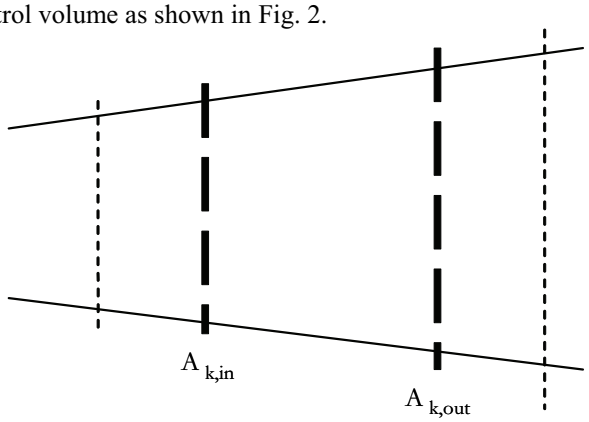

Figure 2. Effective wall bounds for phase k

These two surfaces close the *k* phase control volume when all bubbles present at the walls are in contact. Let us denote by *L* the distance between these two cross sections. These intermediate surfaces are related to the fluid control volume surfaces by

$$\frac{A_{k,out} - A_{k,in}}{L} = \frac{A_{i+1/2} - A_{i-1/2}}{\Delta x}.$$

Consequently,

$$A_{k,out} - A_{k,in} = \frac{L}{\Delta x}(A_{i+1/2} - A_{i-1/2}).$$

Assuming the two phase mixture homogenous enough

$$\frac{L}{\Delta x} \cong \alpha_k.$$

Consequently,

$$\int_{S_{sk}} P_k \vec{n} dS = -P_k \alpha_k (A_{i+1/2} - A_{i-1/2}) \vec{i}.$$

The **solid surface integral** is thus

$$\int_{S_s} X_k \begin{pmatrix} 0 \\ \rho\vec{u} \\ \rho\vec{u} \otimes \vec{u} + P\overline{I} \\ (\rho E + P)\vec{u} \end{pmatrix} \cdot \vec{n} dS = \begin{pmatrix} 0 \\ 0 \\ -P_k \alpha_k (A_{i+1/2} - A_{i-1/2}) \vec{i} \\ 0 \end{pmatrix}. \qquad (6)$$

The fluid surface integral

$$\int_{S_f} X_k F \cdot \vec{n} dS$$

has now to be considered. Consider for example the inflow cross-section $A_{i-1/2}$. We thus have to compute

$$\int_{A_{i-1/2}} X_k F \cdot \vec{n} dS.$$

The inflow and outflow sections are perfectly determined, for example with relations like

$$A_{i-1/2} = \min(A_{i-1}, A_i).$$

Each cross section is partly occupied by a given phase. Indeed, several types of contact are present, as summarized in Table 1 below.

Table 1. Evaluation of convective fluxes at cell boundary i-1/2

Type of Contact	Contact area	Indicator function 1	Convective flux
1-1	$S_{11} = A_{i-1/2}\mathrm{Min}(\alpha_{1,i-1}, \alpha_{1,i})$	$X_1^*(1,1) = 1$	$F^*(1,1)$
1-2	$S_{12} = A_{i-1/2}\mathrm{Max}(\alpha_{1,i-1} - \alpha_{1,i}, 0)$	$X_1^*(1,2) = \begin{cases} 1 \text{ if } u^*(1,2) > 0 \\ 0 \text{ otherwise} \end{cases}$	$F^*(1,2)$
2-1	$S_{21} = A_{i-1/2}\mathrm{Max}(\alpha_{1,i} - \alpha_{1,i-1}, 0)$	$X_1^*(2,1) = \begin{cases} 1 \text{ if } u^*(2,1) < 0 \\ 0 \text{ otherwise} \end{cases}$	$F^*(2,1)$
2-2	$S_{22} = A_{i-1/2}\mathrm{Min}(\alpha_{2,i-1}, \alpha_{2,i})$	$X_1^*(2,2) = 0$	$F^*(2,2)$

The **fluid integral** is thus obtained, using Table 1 as

$$\int_{A_{i-1/2}} X_1 F \cdot \vec{n} dS = \sum_{lm} S_{lm} X_1^*(l,m) F^*(l,m). \qquad (7)$$

It remains to compute the last integral associated to interaction effects,

$$\int_V (F - \vec{u}_I U) grad(X_k) dV.$$

For the sake of simplicity we consider only this integral at cell boundaries, where volume fraction jumps are present. Inside the control volume we already know that these terms correspond to relaxation terms, that have been determined previously (see [5] for example) and are here incorporated.

We now note that at each point where $grad(X_k)$ is non zero, the difference $(F - \vec{u}_I U)$ is necessarily locally constant (this difference correspond to the Rankine Hugoniot conditions, or interface conditions in the present context). Therefore, the volume integral (here a surface integral, as we consider a 2D flow) transforms to

$$\int_V (F - \vec{u}_I U) grad(X_k) dV = \int_S (F - \vec{u}_I U) grad(X_k) dS$$

(where we have changed notations, S is V in two dimensions), or

$$\int_S (F - \vec{u}_I U) grad(X_k) dS = \int_{x_{i-1/2}-\varepsilon}^{x_{i-1/2}+\varepsilon} \int_{y=-0.5H_{i-1/2}}^{0.5H_{i-1/2}} (F - \vec{u}_I U) grad(X_k) dxdy + \int_{x_{i+1/2}-\varepsilon}^{x_{i+1/2}+\varepsilon} \int_{y=-0.5H_{i+1/2}}^{0.5H_{i+1/2}} (F - \vec{u}_I U) grad(X_k) dxdy$$

Here two integrals only are present because internal bubbles are treated as relaxation terms, as stated above. The two integrals correspond to the two boundary surfaces.

We now transform one of these surface integrals into a contour integral, by using the fact that the interface conditions are locally constant,

$$\int_S (F-\vec{u}_I U)\,grad(X_k)\,dS = \int_{x_{i-1/2}-\varepsilon}^{x_{i-1/2}+\varepsilon}\int_{y=-0.5H_{i-1/2}}^{0.5H_{i-1/2}} (F-\vec{u}_I U)\,grad(X_k)\,dxdy + \int_{x_{i+1/2}-\varepsilon}^{x_{i+1/2}+\varepsilon}\int_{y=-0.5H_{i+1/2}}^{0.5H_{i+1/2}} (F-\vec{u}_I U)\,grad(X_k)\,dxdy$$

where $\varepsilon \to 0^+$. We now focus on one of these two integrals

$$\int_{x_{i-1/2}-\varepsilon}^{x_{i-1/2}+\varepsilon}\int_{y=-0.5H_{i-1/2}}^{0.5H_{i-1/2}} (F-\vec{u}_I U)\,grad(X_k)\,dxdy$$

$$= (F-\vec{u}_I U)_{i-1/2}\int_{x_{i-1/2}-\varepsilon}^{x_{i-1/2}+\varepsilon}\int_{y=-0.5H_{i-1/2}}^{0.5H_{i-1/2}} grad(X_k)\,dxdy \qquad (8)$$

$$= (F-\vec{u}_I U)_{12,i-1/2}\left[X_k\right]_{12} S_{12} + (F-\vec{u}_I U)_{21,i-1/2}\left[X_k\right]_{21} S_{21}$$

Where the $\left[X_k\right]_{lm}$ and S_{lm} are obtained from the Table 2 below.

Table 2. Evaluation of Lagrangian fluxes at cell boundary i-1/2.

Type of Contact	Surface of Contact	Jump of the indicator function 1	Lagrangian flux
1-1	$S_{11} = A_{i-1/2}\mathrm{Min}(\alpha_{1,i-1},\alpha_{1,i})$	$[X_1^*](1,1) = 0$	$F^{lag,*}(1,1)$
1-2	$S_{12} = A_{i-1/2}\mathrm{Max}(\alpha_{1,i-1}-\alpha_{1,i},0)$	$[X_1^*](1,2) = \begin{cases} -1 \text{ if } u_1^*(1,2) > 0 \\ 0 \quad \text{otherwise} \end{cases}$	$F^{lag,*}(1,2)$
2-1	$S_{21} = A_{i-1/2}\mathrm{Max}(\alpha_{1,i}-\alpha_{1,i-1},0)$	$[X_1^*](2,1) = \begin{cases} 1 \text{ if } u_1^*(2,1) > 0 \\ 0 \quad \text{otherwise} \end{cases}$	$F^{lag,*}(2,1)$
2-2	$S_{22} = A_{i-1/2}\mathrm{Min}(\alpha_{2,i-1},\alpha_{2,i})$	$[X_1^*](2,2) = 0$	$F^{lag,*}(2,2)$

Equations Summary

Substituting Eqns. (5), (6), (7), and (8) into Eqn. (4) gives

$$\frac{\partial V\langle X_k U\rangle}{\partial t} + \frac{\left\{\sum_{lm} S_{lm} X_1^*(l,m) F^*(l,m)\right\}_{i+\frac{1}{2}} - \left\{\sum_{lm} S_{lm} X_1^*(l,m) F^*(l,m)\right\}_{i-\frac{1}{2}}}{\Delta x} = \frac{\left\{(F-\vec{u}_I U)_{12}\left[X_k\right]_{12} S_{12} + (F-\vec{u}_I U)_{21}\left[X_k\right]_{21} S_{21}\right\}_{i-\frac{1}{2}}}{\Delta x} + \frac{\left\{(F-\vec{u}_I U)_{12}\left[X_k\right]_{12} S_{12} + (F-\vec{u}_I U)_{21}\left[X_k\right]_{21} S_{21}\right\}_{i+\frac{1}{2}}}{\Delta x} + \begin{pmatrix} 0 \\ 0 \\ P_k \alpha_k \left(\dfrac{A_{i+\frac{1}{2}} - A_{i-\frac{1}{2}}}{\Delta x}\right) \\ 0 \end{pmatrix} \qquad (9)$$

or

$$\frac{\partial \alpha_k A U}{\partial t} + \frac{\Delta(\alpha_k A F)}{\Delta x} = \frac{F^{lag} A \Delta\alpha}{\Delta x} + \begin{pmatrix} 0 \\ 0 \\ P_k \alpha_k \left(\dfrac{A_{i+\frac{1}{2}} - A_{i-\frac{1}{2}}}{\Delta x}\right) \\ 0 \end{pmatrix}$$

This augmented Euler fluid equation system is solved numerically with an explicit Euler time integration and an approximate Riemann solver, the HLLC scheme [6], to give the flux values at cell interfaces.

From a theoretical standpoint it can be useful to identify the continuous equation system resulting from the discrete equation system. By taking the limit as spatial and time step sizes become small and employing the acoustic Riemann problem, the equivalent continuous system (with the reinsertion of relaxation terms and very much simplified heat and mass

transfer model between the phases) can be written from the discrete equation system above as follows:

Volume fraction

$$\frac{\partial \alpha_k}{\partial t} + u_I \frac{\partial \alpha_k}{\partial x} = \mu\left(P_k - P_j\right) + \frac{\Gamma_k}{\rho_I}$$

Mass

$$\frac{\partial \alpha_k \rho_k A}{\partial t} + \frac{\partial \alpha_k \rho_k u_k A}{\partial x} = \Gamma_k$$

Momentum

$$\frac{\partial \alpha_k \rho_k u_k A}{\partial t} + \frac{\partial \alpha_k A(\rho_k u_k{}^2 + P_k)}{\partial x} = P_I A \frac{\partial \alpha_k}{\partial x} + P_k \alpha_k \frac{\partial A}{\partial x} + \lambda\left(u_I - u_k\right) + \Gamma_k u_I$$

or

$$\frac{\partial \alpha_k \rho_k u_k A}{\partial t} + \frac{\partial \alpha_k A \rho_k u_k{}^2}{\partial x} + \alpha_k A \frac{\partial P_k}{\partial x} = (P_I - P_k) A \frac{\partial \alpha_k}{\partial x} + \lambda\left(u_j - u_k\right) + \Gamma_k u_I$$

In the above equations the pressure relaxation coefficient is given by [5]

$$\mu = \frac{S_I}{V} \frac{1}{\left(\rho_{gas} c_{gas} + \rho_{liq} c_{liq}\right)}$$

and the velocity relaxation coefficient is given as

$$\lambda = \mu\left(\rho_{gas} c_{gas}\right)\left(\rho_{liq} c_{liq}\right)$$

where c_k are the phasic sound speeds. The quantity S_I / V is the interfacial area per unit volume or the *specific interfacial area* (SSV).

Some special forms are noted, in particular if A is constant we have the reduced form

$$\frac{\partial \alpha_k \rho_k u_k}{\partial t} + \frac{\partial \alpha_k (\rho_k u_k{}^2 + P_k)}{\partial x} = P_I \frac{\partial \alpha_k}{\partial x} + \lambda\left(u_j - u_k\right) + \Gamma_k u_I .$$

Also, if A varies with α constant (equivalent to single-phase)

$$\frac{\partial \rho_k u_k A}{\partial t} + \frac{\partial A(\rho_k u_k{}^2 + P_k)}{\partial x} = P_k \frac{\partial A}{\partial x} .$$

Energy

$$\frac{\partial \alpha_{liq} \rho_{liq} E_{liq} A}{\partial t} + \frac{\partial \alpha_{liq} (\rho_{liq} E_{liq} + P_{liq}) u_{liq} A}{\partial x} = P_I u_I A \frac{\partial \alpha_{liq}}{\partial x} - P_I \left[\mu\left(P_{liq} - P_{gas}\right) - \frac{\Gamma}{\rho_I}\right] + u_I \left[\lambda\left(u_{gas} - u_{liq}\right)\right] - \Gamma e_I + \dot{Q}$$

$$\frac{\partial \alpha_{gas} \rho_{gas} E_{gas} A}{\partial t} + \frac{\partial \alpha_{gas} (\rho_{gas} E_{gas} + P_{gas}) u_{gas} A}{\partial x} = P_I u_I A \frac{\partial \alpha_{gas}}{\partial x} + P_I \left[\mu\left(P_{liq} - P_{gas}\right) - \frac{\Gamma}{\rho_I}\right] - u_I \left[\lambda\left(u_{gas} - u_{liq}\right)\right] + \Gamma\left(e_I - h_{gas-liq}\right)$$

where

$$\dot{Q} = h\left(T_{gas} - T_{liq}\right), \quad \Gamma = \dot{Q} / h_{gas-liq}$$

and $h_{gas-liq}$ is the latent heat of vaporization. These simple (not necessarily physically correct, but still exhibiting a qualitatively similar effect) mass and heat transfer models are added for a first look at their effects. Of course the latent heat of vaporization term will be absent when a correct phase change model is employed.

RESULTS AND CONCLUSIONS

In the following we first present results for a single phase, 1-dimensional variable area simulation with the compressible Euler equations using a stiffened gas equation of state SGEOS

$$P = (\gamma - 1)\rho(e - q) - \gamma P_\infty \qquad (10)$$

where γ, q, and P_∞ are material (fluid) constants. Here q is a "binding" energy which for two-phase flow will effectively represent a reference state. The SGEOS can be used for compressible gas and compressible liquid phases with appropriate selection of these constants for each phase [7]. This 1-D, volume-centered, finite volume method uses the HLLC approximate Riemann solver to determine the fluxes at cell faces. The scheme uses explicit time stepping to integrate the solution to steady state. This steady state solution is used as an initial benchmark solution for the initial two phase DEM results (described next).

Fig. 3 shows the nozzle area distribution used in all the simulations examined in this study. Fig. 4 shows the simulation results from a single-phase code using the same explicit HLLC method for a compressible liquid phase. The plots show steady-state density, velocity, pressure and Mach number distributions. These results are presented for comparison to those of particular two-phase DEM simulations and are considered a preliminary or initial benchmark case. Notice that pressure exhibits negative values here. This is to be expected because we are not allowing phase change to occur. The SGEOS permits negative pressure by as much as $-\gamma P_\infty$ for density or internal energy sufficiently small; this is to be expected.

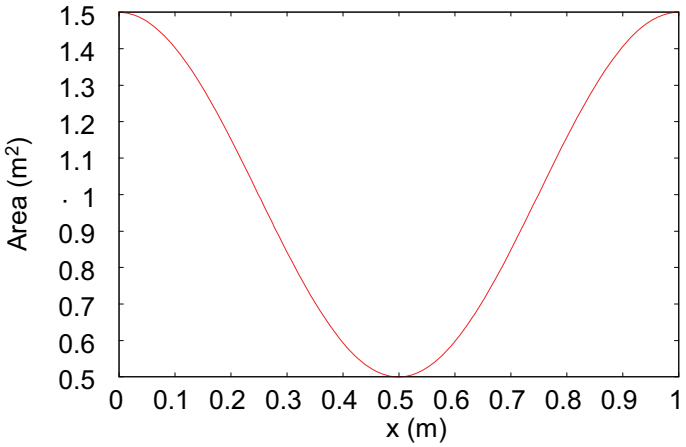

Figure 3. Nozzle area distribution used for all simulations

The DEM two phase method is then employed with this same compressible liquid (water) and with a compressible gas (water vapour). Again the SGEOS is used for each phase [7]. First relaxation is turned off which means that the phases do not interact with each other. That is two independent, variable area solutions should evolve, one for each phase. The volume fractions should not change. The solution for the liquid phase should be identical to the single phase result presented in Fig. 4. The results from this case are presented in Fig. 5. Comparison of the plots of density, velocity, pressure and Mach number between Figs. 4 and 5 show the results are identical lending confidence to our implementation of the discrete equation method. Not shown is the volume fraction which remained constant as was expected. The results from a compressible gas single-phase simulation are not shown but were also identical to a benchmark solution for that phase.

Then two different degrees of relaxation are turned on via specification of the specific interfacial area (SSV), i.e. interfacial area per unit volume. Results for SSV=1 are shown in Figs. 6 and 7 for liquid and gas respectively while results for SSV=100 are shown in Figs. 8 and 9. These results show that the method is capable of resolving shock waves. Also the interaction between the two phases is not sufficient to relax the pressure to the same value for both. The liquid pressure is again negative because no phase change is permitted. In Figs. 6 and 7 it is seen that with a stronger interaction between the two phases, the liquid pressure is not as strongly negative as in the previous case and the gas phase is slowed down due to the drag between the two phases such that no shock waves are present.

Finally, relaxation is maintained (SSV=100) and the simple mass and heat transfer models (as noted above) are added for a first look at their effects. Results for each phase are shown in Figs. 10 and 11. Liquid pressure still has small negative non-equilibrium values because mass transfer rate is limited.

In this paper we have outlined the construction of a DEM model for 1-D flow of two compressible phases in ducts of spatially variable cross-section to test this approach. For the first time, we have demonstrated on a converging-diverging two-phase nozzle that this well-posed 2-pressure, 2-velocity model can be integrated to a meaningful steady-state with both phases treated as compressible. We have included a crude, though simple, mass transfer model. In the future we will investigate use of general mass transfer between multiple compressible phases through development of a Reactive Riemann solver (RDEM) and the incorporation of fully implicit time integration to facilitate efficient computation of slow transients.

ACKNOWLEDGMENTS

The authors acknowledge the US Department of Energy, Office of Nuclear Energy, for funding this research through the Laboratory Directed Research and Development program at the Idaho National Laboratory under DOE Idaho Operations Office Contract DE-AC07-05ID14517.

REFERENCES

[1] R. Abgrall, R. Saurel, "Discrete equations for physical and numerical compressible multiphase mixtures," *J. Comp. Phys.* **186** (2003) 361-396.

[2] O. Le Métayer, J. Massoni, R. Saurel, "Modeling evaportation fronts with reactive Riemann solvers," *J. Comp. Phys.* **205** (2005) 567-610.

[3] R.A. Berry, R. Saurel, F. Petitaps, E. Daniel, O. Le Métayer, S. Gavrilyuk, N. Dovetta, R.C. Martineau, *Progress in the development of compressible, multiphase flow modeling capability for nuclear reactor flow,* Idaho National Laboratory report INL/EXT-08-15002, Oct. 2008.

[4] R.J. Leveque, *Finite Volume Methods for Hyperbolic Problems*, Cambridge Univ. Press 2002.

[5] A. Chinnayya, E. Daniel, R. Saurel, "Modelling detonation waves in heterogeneous energetic materials," *J. Comp. Phys.* **196** (2004) 490-538.

[6] E.F. Toro, *Riemann Solvers and Numerical Methods for Fluid Dynamics*, 2nd Edition, Springer, 1999.

[7] O. Le Métayer, J. Massoni, R. Saurel, "Elaborating equations of state of a liquid and its vapor for two-phase flow models," (in French) *Int. J. Thermal Hydraulics* **43** (2004) 265-276.

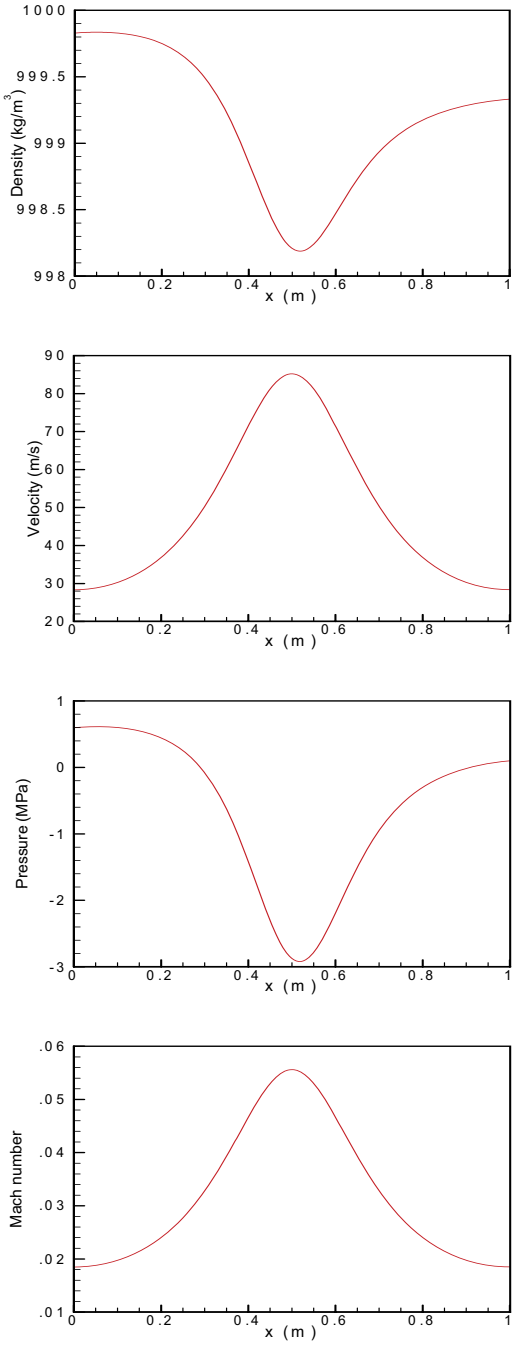

Figure 4. Liquid phase results from single-phase code.

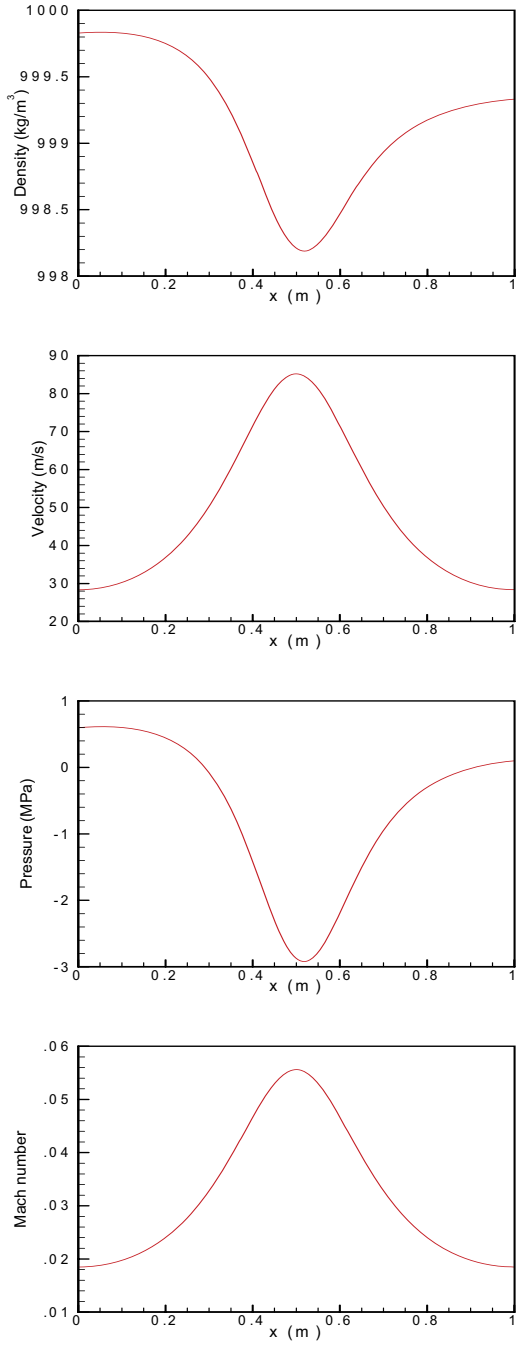

Figure 5. Liquid phase results from two-phase code with no relaxation.

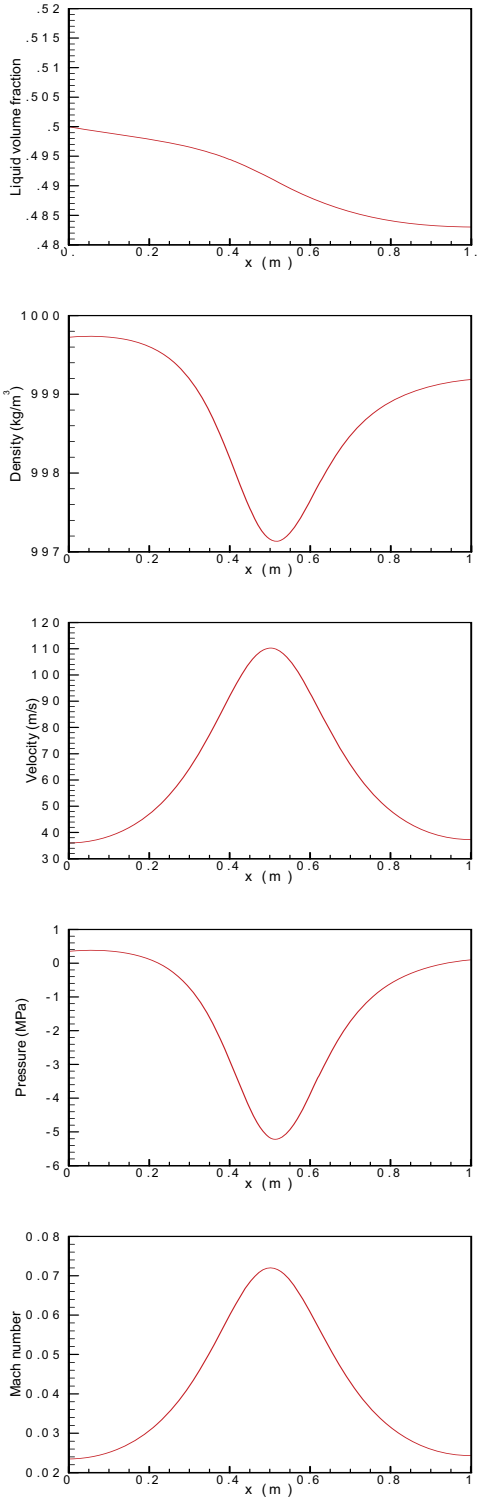

Figure 6. Liquid phase results from two-phase code with relaxation (SSV=1).

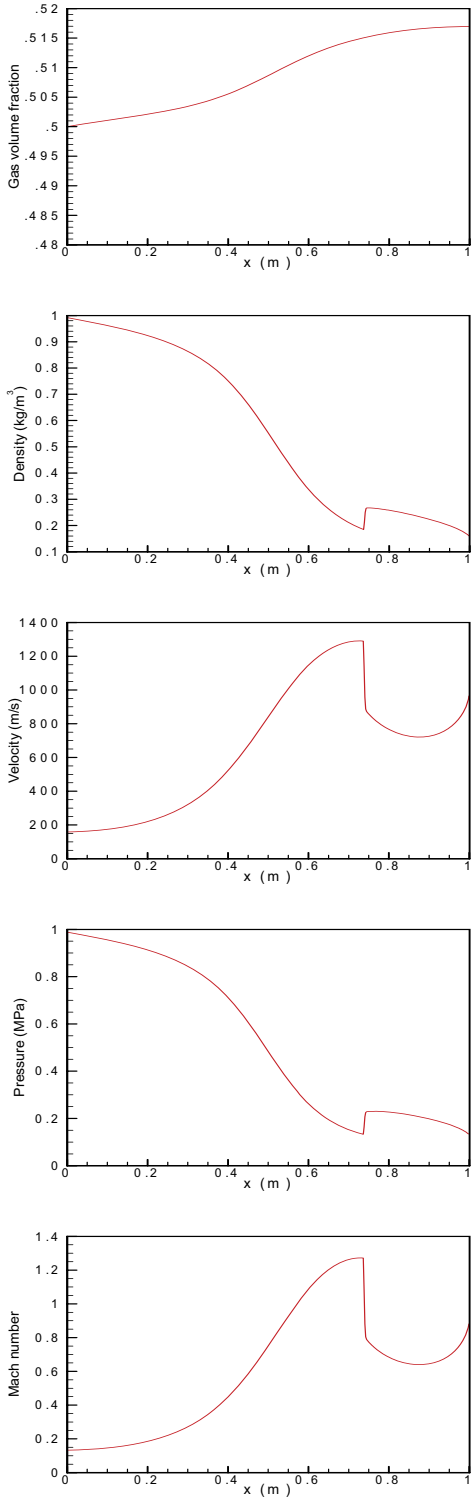

Figure 7. Gas phase results from two-phase code with relaxation (SSV=1).

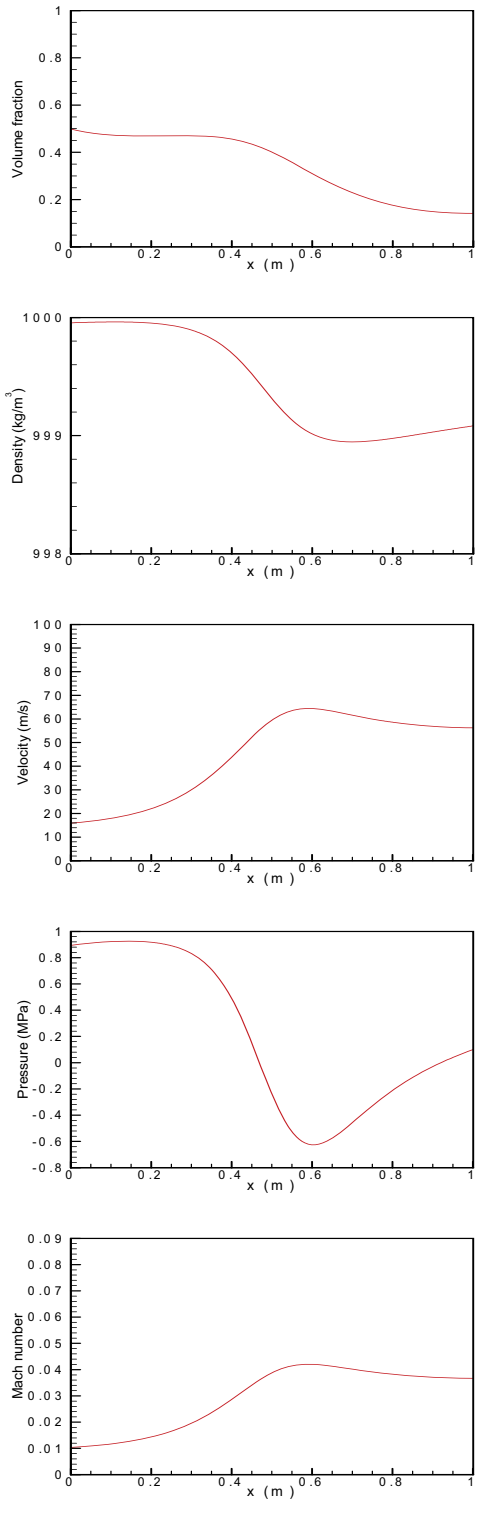

Figure 8. Liquid phase results from two-phase code with relaxation (SSV=100).

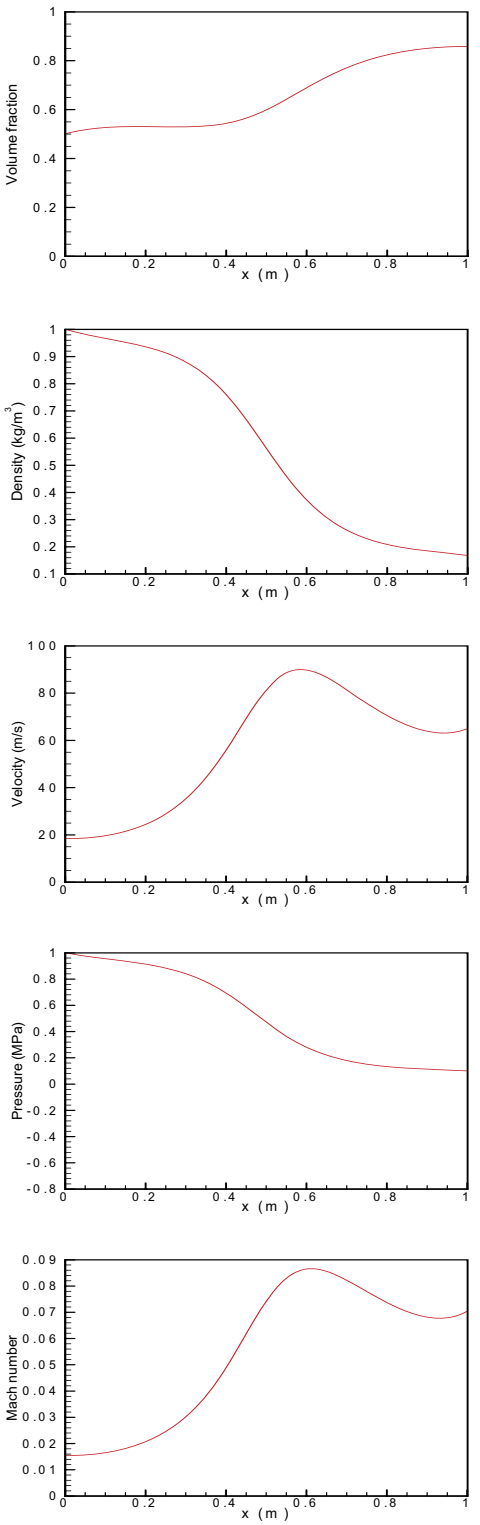

Figure 9. Gas phase results from two-phase code with relaxation (SSV=100).

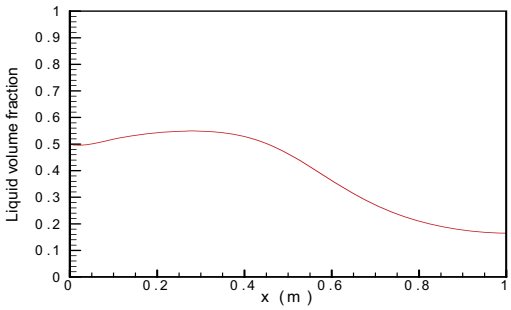

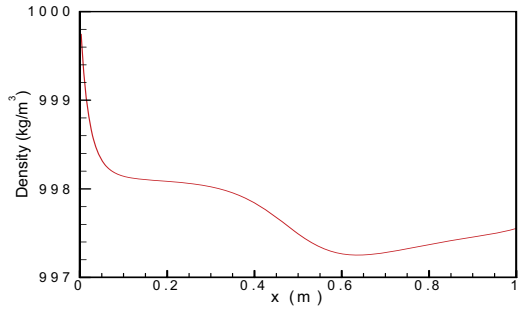

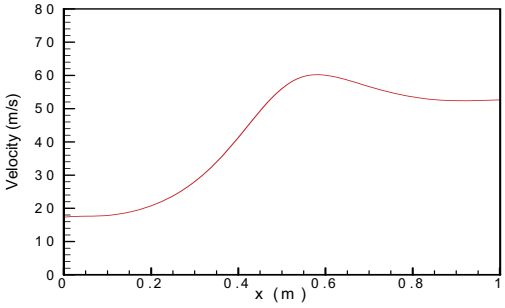

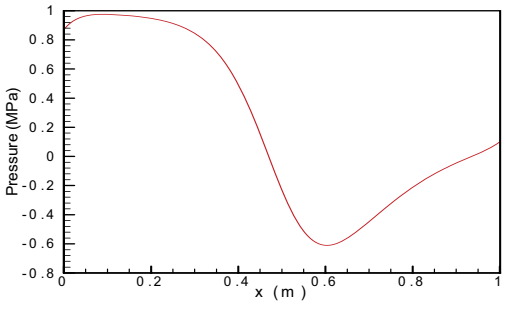

Figure 10. Liquid phase results from two phase code with heat and mass transfers and relaxation (SSV=100).

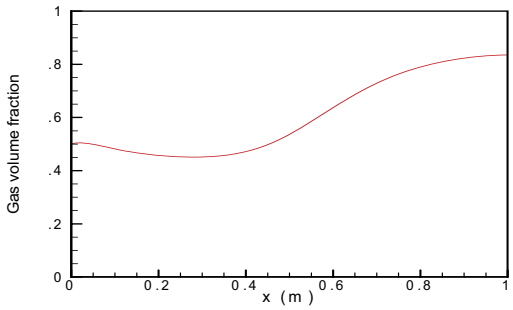

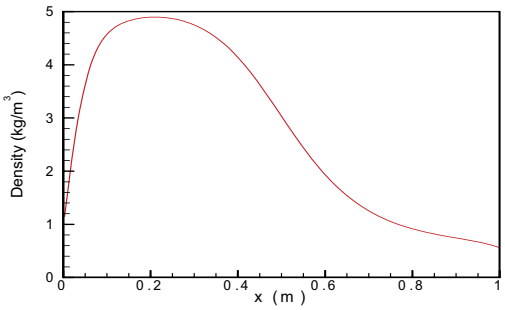

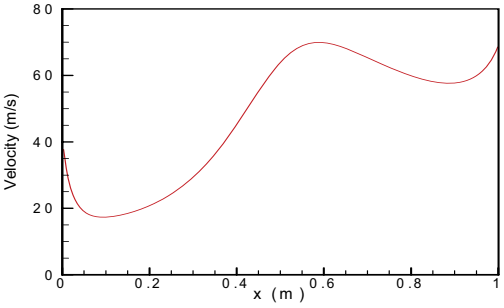

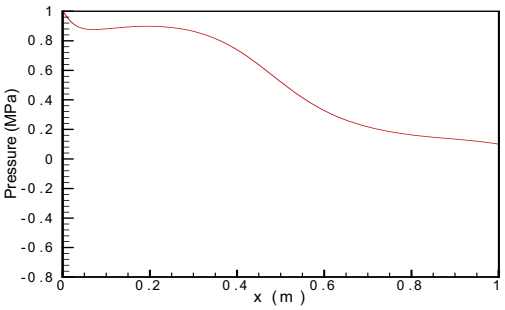

Figure 11. Gas phase results from two phase code with heat and mass transfers and relaxation (SSV=100).